Journal of Applied Polymer Science

Development of Quasi-Solid-State Dye-Sensitized Solar Cell Based on an Electrospun Polyvinylidene Fluoride–Polyacrylonitrile Membrane Electrolyte

Malaisamy Sethupathy, Priyanka Pandey, Paramasivam Manisankar
Department of Industrial Chemistry, Alagappa University, Karaikudi 630 003, Tamil Nadu, India
Correspondence to: P. Manisankar (E-mail: pms11@rediffmail.com)

ABSTRACT: Dye sensitized solar cell (DSSC) has been magnetizing more awareness in current research due to more efficiency. The foremost drawback of the solar cell is the evaporation of organic electrolyte. In order to address this problem, the polyvinylidene fluoride–polyacrylonitrile–Electrospinning Fibrous Membranes were prepared by electrospinning method and the photovoltaic performances were evaluated. The polyvinylidene fluoride and polyacrylonitrile were mixed in *N,N′*-dimethylformamide and acetone at an applied potential of 15 kV. The surface morphology of membrane is interconnected with network structure and a large number of voids were observed from Field Emission Scanning Electron Microscopy images. The electrolyte uptakes up to 310% were observed and it shows an increase in the ionic conductivity up to 6.12×10^{-2} S cm^{-1} at 25°C. The fabricated DSSCs show open circuit voltage (V_{oc}) of 0.74 V, fill factor (FF) of 0.65 and short circuit current (J_{sc}) of 6.20 mA cm^{-2} at an incident light intensity of 100 mW cm^{-2}. The photovoltaic efficiency also reached up to 3.09%. © 2013 Wiley Periodicals, Inc. J. Appl. Polym. Sci. **2014**, *131*, 40022.

KEYWORDS: electrospinning; fibers; optical and photovoltaic applications; morphology

Received 16 June 2013; accepted 29 September 2013
DOI: 10.1002/app.40022

INTRODUCTION

The renewable energy sources are the need of the hour for the human society because of limited availability of fossil fuels. The necessity for a substantial expansion of renewable energy sources for next generation, principally solar energy, has been budding constantly with increasing speed.[1] The dye-sensitized solar cells (DSSCs) using organic liquid electrolytes have received significant intensive interest since their beginning because of their higher efficiency, lower production cost, simple structure, higher power conversion efficiency, and easy fabrication procedure compared with silicon solar cells.[2,3] The main purpose of solar cells is to convert directly solar energy into electrical energy and it can produce electricity without extraordinary maintenance and environmental anxieties. Previously silicon-based inorganic solar cells have been used for the same process, but the major disadvantages of this type of solar cells are higher initial costs and an unwieldy fabrication process. Therefore, a great effort is in progress to develop solar cells that consist of more easily processed and low-cost materials. In this effort, DSSCs with different polymer electrolytes such as PEO, PMMA, and PEO-PVdF were fabricated and studied.[4–6]

First of all, Gratzel group reported dye-sensitized solar cells (DSSCs) with 12% of power conversion efficiency (PCE) that has gained much attention[2] due to the usage of a liquid electrolyte which is very close to those of amorphous silicon-based inorganic solar cells.[7,8] But reduction of liquid electrolyte either by leakage or evaporation is the main drawback of this system which restricted the long-term stabilities of DSSCs. In order to overcome these problems associated with the use of liquid electrolytes in DSSCs, alternatives such as inorganic or organic hole conductors,[9] polymer gel electrolytes,[10] and ionic liquids[11] have been tried. In recent times, quasi-solid-state DSSCs utilizing polymer gel electrolytes have received increasing attention due to their non-flammable character, negligible vapor pressure, good permeability into the mesoporous TiO_2, and high ionic conductivity.[1] Mostly, popular polymer gel electrolytes, for example polyacrylonitrile (PAN),[12] poly(ethylene glycol) (PEG),[13] poly(methyl methacrylate) (PMMA),[14] poly(MMA-*co*-MAA)/PEG, cyanoacrylate, poly(oligoethylene glycol methacrylate), polyvinylideneflouride (PVdF), poly(siloxane-*co*-ethyleneoxide), poly(butyl acrylate), poly(vinylidene fluoride-*co*-hexafluoropropylene) (PVdF-HFP), and poly(oligoethylene glycol methacrylate) (POEGM),[15] with different plasticizers have been used in quasi-solid-state DSSCs. The PVdF is considered as a good base for electrolyte due to its high dielectric constant ($e = 8.4$), good electrochemical stability, affinity towards liquid electrolyte solutions because of electron withdrawing fluorine atoms (–C–F) in the backbone structure

and exhibits ionic conductivities in the range of 10^{-4} to 10^{-3} S cm^{-1} at room temperature.[16] The film based on PVdF exhibited higher conductivity and higher degree of crystallinity. The crystalline part of PVdF hinders the free migration of Li^+ ions and hence PVdF-based electrolytes have lower evaporation. These properties of PVdF are helpful in breaking the lithium salt to lithium ions while transforming into a polymer electrolyte. PAN has attractive individuality such as thermal constancy, high-quality ionic conductivity, and excellent morphology for electrolyte uptake and good compatibility with liquid electrolyte. The PAN having –CN groups easily make bond with –C=O groups of the liquid electrolytes propylene carbonate (PC) or ethylene carbonate (EC) and also with Li^+ ions.[16] Previous results from nuclear magnetic resonance, differential scanning calorimetry, Fourier Transform Infrared spectroscopy studies on PAN-based electrolytes demonstrate the interactions between the groups in PC or EC and PAN.[17,18] It is clear from the reported literatures that PVdF and PAN are independently having advantageous characteristics as a host polymer in polymer electrolytes. Furthermore, in a group, both the polymer electrolytes share some important characteristics which could not be derived from PVdF or PAN. Since PVdF and PAN performing well independently as host polymer in polymer electrolyte, the composites of the two are expected to have better performance due to synergetic effect.

Electrospinning process is multipurpose, easy to handle and cost-effective novel technique that develops an electrostatic force to produce nanofibers in the range of a few 100 nm to a few microns. It is a very promising and versatile technique because it facilitates the production of multifunctional nanofibers from various polymers, polymer blends, sol–gels, composites, ceramics, and etc.[19] The prepared electrospun nanofibers have several significant functional characteristics such as a large surface area, pore size within the nano range, distinctive physical and mechanical properties along with the design flexibility for chemical/physical surface functionalization. It is applicable in a number of areas such as medicine, biotechnology, tissue-engineering, membrane filtration technologies, textile, and fabrication of DSSCs.[1,19] The most important advantage of the electrospinning process is coupled with the high degree of control that is responsible over morphology, porosity, and composition using simple equipment. The main characteristics of electrospinning is to generate dry fibrous membranes by rapid evaporation of the solvent, which could help in phase mixing between PVdF and PAN or avoid the phase separation because both the electrolytes are partially miscible. Therefore, electrospinning process was specifically selected for the generation of uniform microporous membranes.[19] Therefore, the working conditions of electrospinning like high voltage, fast evaporation, and uniform fiber formation would stimulate the phase mixing between PVdF and PAN electrolytes and finally a miscible composite of PVdF and PAN could be formed as a porous fibrous membrane.[20] Thus electrospinning method has been proposed for the preparation of PVdF–PAN composites. The significance of this study lies in the preparation of more fibrous PVdF–PAN membranes by electrospinning method and utilization of these membranes as polymer host in the preparation of polymer electrolyte. By introducing this type of newer approach, the performance of the polymer electrolyte would increase the efficiency of the DSSC fabricated.

In this investigation, PVdF–PAN electrospun fibrous membranes (PVdF–PAN-ESFMs) were prepared and evaluated their behavior such as electrolyte uptake, porosity calculation of the electrospun polymer blend nanofibers, ionic-conductivity by impedance measurement, morphological measurement by scanning electron microscope (SEM), presence of active functional group by Fourier Transfer Spectroscopy (FTIR), and crystallinity by X-ray diffraction pattern (XRD). Their photovoltaic performance (*I–V*) evaluations for the fabricated DSSCs have also been studied.

EXPERIMENTAL

Materials

Polyvinylidene fluoride (PVdF; $M_w = 3{,}00{,}000$), polyacrylonitrile (PAN; $M_w = 1{,}50{,}000$), *N,N′*-dimethylformamide (DMF), iodine (I_2), lithium iodide (LiI), 0.3 m*M* anhydrous ethanolic solution of N719 dye ($[(C_4H_9)_4N]_2[Ru(II)L_2(NCS)_2]$), where L = 2,2′-bipyridyl-4,4′-dicarboxylic acid, rutheniumTBA535, acetone, propylene carbonate (anhydrous, 99.7% and the water content is <0.002%), and fluorine-doped tin oxide (FTO) glass (15 Ω s^{-2}) were purchased from Sigma-Aldrich. All reagents and chemicals were used without further purification.

Electrospun PVdF–PAN Composite (PVdF–PAN-ESFM) Nanofiber Preparation

Figure 1 shows the photographic image of the electrospinning instrument. Three main components such as: (a) Power unit—a high voltage supplier, (b) Feeding unit—a capillary tube with stainless steel needle of a small diameter, and (c) Collection unit—drum collector wrapped with aluminum foil are present. Once it has been driven out from the needle with a small hole, the polymer solution was introduced into the applied electric field. The polymer string was formed between two electrodes bearing opposite electrical charges. Before the polymer solutions reach the collector, the excess solvents were evaporated in the jet and were collected as an interconnecting web of small fibers. One of these electrodes was placed into the solution and the other onto a collector. Electrospun PVdF–PAN nanofibers were prepared from a 10 wt % solution of PVdF (7.5 g)—PAN (2.5 g) dissolved in mixture of acetone/*N,N*-dimethylacetamide (7 : 3 v/v %) for 24 h at room temperature. Further, this polymer solution was filled in to the 10 mL stainless steel syringe (needle-24 G) using a syringe pump (KD Scientific, model 100), and a high voltage of 20 kV with a mass flow rate of 1.5 mL h^{-1} was applied to the end of the needle. The distance between the nozzle of the syringe and the collector (aluminum drum) was 15 cm at 25°C. Thus after the completion of electrospinning, the dry nanofiber accumulated on the collector. Then fibrous membranes were carefully peeled off from the aluminum foil after drying in the vacuum oven at 60°C for 12 h.

Characterization of the PVdF–PAN-ESFM

The morphology of the electrospun PVdF–PAN nanocomposite membrane was observed using field-enhanced scanning electron microscopy (FEI, Quanta 250) under vacuum condition. The sample was gold-sputtered prior to the SEM measurement. The average diameter of nanofibers was determined by analyzing the SEM images with an image analyzing Gwydion 2.28 software. The crystallinity of PVdF–PAN-ESFM was evaluated by

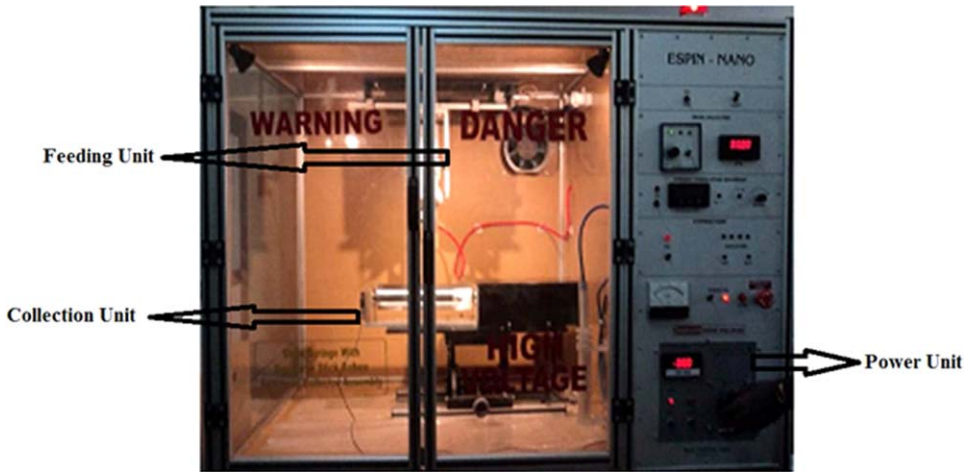

Figure 1. Photographic diagram of the electrospinning method. [Color figure can be viewed in the online issue, which is available at wileyonlinelibrary.com.]

computer controlled X-ray diffraction (XRD) system (X'Pert PRO PAN anlytical diffractometer) with Cu $K\alpha$ radiation at 40 kV/30 mA. The diffractograms were scanned in a 2θ range of 10–70 at a rate of 2 min^{-1}. Moreover, the crystallinity of nanofiber membrane was determined by a peak deconvolution method.[21] The diffraction peak at $2\theta = 20.55$ and 23.0 were shifted into amorphous to crystalline region by a curve fitting techniques. The crystallinity is defined as the area of crystalline phase divided by the total area of crystalline phase and amorphous phases as described in eq. (1):

$$\text{crystalinity}\,(\%) = \frac{A_c}{A_c + A_a} \times 100 \tag{1}$$

where A_c is the area of the crystalline phase and A_a is the area of the amorphous phase.

Fourier transform infrared spectroscopy (FTIR) recorded in KBr pellets using Nicolet 5700 spectrophotometer (Thermo Electron Co.) in the wave number range 400–4000 cm^{-1} revealed the presence of functional group in PVdF, PAN, and PVdF–PAN-ESFM nanofiber membrane.

Estimation of PVdF–PAN–ESFM Electrolytes Characteristics

PVdF–PAN-ESFMs were soaked into 0.6*M* 1-hexyl-2,3-dimethylimidazolium iodide, 0.1*M* LiI, 0.05*M* I_2, and 0.5*M* 4-*tert*-butylpyridine in EC : PC (1 : 1 wt %) to obtain the corresponding electrospun PVdF–PAN membrane electrolyte at room temperature. The % of electrolyte uptake of ESFMs was determined by soaking the membranes in liquid electrolyte solution and measuring the changes in mass of the membranes. The electrolyte uptake was calculated using the eq. (2).[22]

$$\text{Electrolyte uptake}\,(\%) = \frac{M_{\text{wet}} - M_{\text{dry}}}{M_{\text{dry}}} \times 100\% \tag{2}$$

where M_{wet} and M_{dry} are mass of membranes after and before soaking in the liquid electrolyte, respectively.

Porosity Percentage Calculation

The pore size of the electrospun nanofiber membranes determined the electrolyte uptake property for the same. The porosity percentage of PVdF–PAN-ESFMs can be determined using *n*-butanol uptake. For this purpose, PVdF–PAN-ESFM was soaked in *n*-butanol for 2 h. The mass of PVdF–PAN-ESFMs before and after immersion was measured. The porosity % of the membrane was calculated using the eq. (3):

$$\text{Porosity}\,(\%) = \frac{m_a/p_a}{m_a/p_b + m_b/p_a} \times 100 \tag{3}$$

where m_a and m_b are the mass of membranes after and before soaking in *n*-butanol, ρ_b and ρ_a are the density of the polymer and *n*-butanol, respectively.

Impedance Measurement for PVdF–PAN-ESFMs

The ion conductivity for PVdF–PAN-ESFM was measured using the "Frequency response analyzer (FRA; Autolab PGSTAT 30, the Netherlands)." The electrospun PVdF–PAN-ESFM was immersed in liquid electrolyte solution (1 : 1 v/v) for 60 min.[23] After that the PVdF–PAN-ESFMs was sandwiched between two symmetrical stainless-steel blocking electrodes. Using an FRA1260 frequency response detector, the resistance of the polymer electrolyte was measured. The frequency ranged from 10 mHz to 5 MHz and the ac amplitude was 10 mV at room temperature. The data was analyzed by Z-plot software.

The ionic conductivity was calculated using the following eq. (4):

$$\sigma = \frac{l}{RA} \tag{4}$$

where σ = ionic conductivity; l = thickness of the film; R = bulk resistance of the electrolyte; and A = the area of the film respectively

Fabrication of DSSC Devices

The fabrication of DSSCs involved the impregnation of dye on TiO_2 and it is used as a working electrode along with Pt counter-electrode. To prepare the working electrode, a thin layer of nonporous TiO_2 film was deposited on a cleaned FTO conducting substrate, using 5% titanium (IV) butoxide in ethanol by spin-coating at 3000 rpm. The TiO_2 paste was spread on the conducting glass substrate using a doctor blade technique followed by annealing at 450°C. The sensitizer N719 dye was

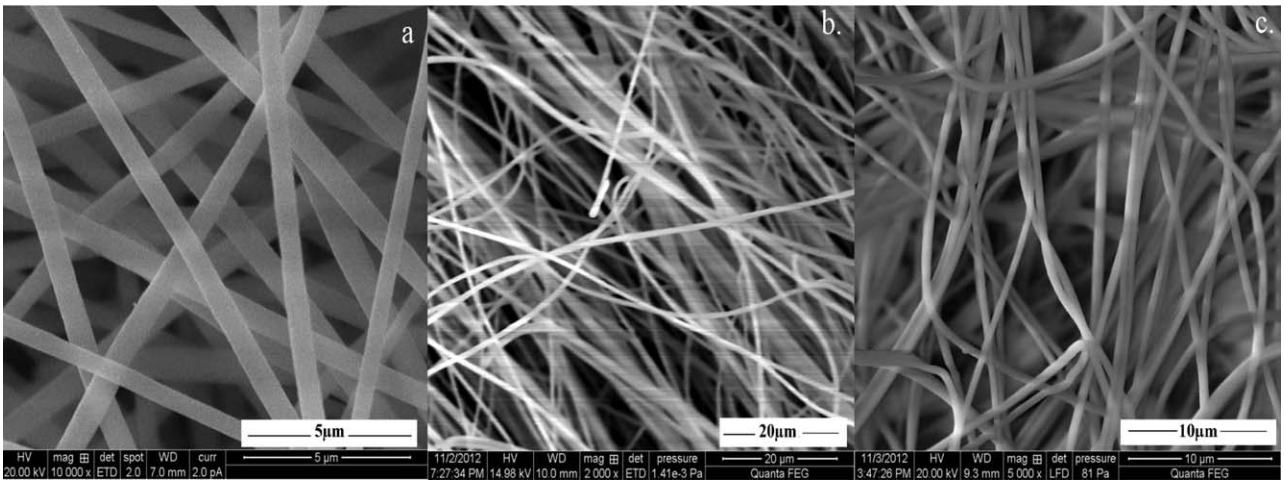

Figure 2. FE-SEM image of electrospun nanofiber membrane: (a) PVdF, (b) PAN, and (c) PVdF–PAN.

dissolved in 0.3 m*M* pure ethanol solution and then TiO_2 deposited FTO was immersed in the dye solution at 25°C for 24 h. Then, the dye-sensitized TiO_2 electrode was rinsed with anhydrous ethanol and dried in moisture free air. The counter electrode was prepared using a drop of 5 m*M* platinic chloride solution (H_2PtCl_6) in 2-propanol, spread on the FTO glass and sintered at 450°C for 30 min followed by drying and annealing. Then it was cooled down from 450 to 25°C at a controlled cooling rate (5°C/min).

The electrospun polymer electrolyte membrane, based on a quasi-solid-state DSSC, was fabricated by sandwiching a piece of the electrospun PVdF–PAN-ESFM between a dye-sensitized TiO_2 working and Pt counter electrode. For comparison, a reference DSSC, based on liquid electrolyte, was fabricated by placing the platinum electrode over the dye-coated TiO_2 electrode. The edges of the cell were sealed with 1 mm wide strips of 60 μm thick Surlyn. A hot press was used to press together the film electrode and the counter electrode. A drop of the liquid electrolyte solution was introduced into the clamped electrodes through one of two small holes drilled in the counter electrode. The holes were then covered and sealed with small squares of Surlyn strip. The resulting cells had an active area of 0.5 cm × 0.5 cm.

I–V Measurement

The photovoltaic performance of the DSSC devices are measured by using the solar simulator (Photo Emission Tech Inc Camarillo, CA 93012, MODEL: 80AAA) at 100 mW cm^{-2} of the light intensity. The exposed area is 0.25 cm^2. The masked area is only 0.05 cm^2. The photoelectron-chemical parameters, i.e., the fill factor (FF) and light-to-electricity conversion efficiency (η), were calculated by the following eqs. (5) and (6):

$$\mathrm{FF} = \frac{V_{max} \times J_{max}}{V_{oc} \times J_{sc}} \tag{5}$$

$$\eta(\%) = \frac{V_{max} \times J_{max}}{P_{in}} \times 100 = \mathrm{FF}\,\frac{V_{oc} \times J_{sc}}{P_{in}} \times 100 \tag{6}$$

where J_{sc} is the short-circuit current density (mA cm^{-2}); V_{oc} is the open-circuit voltage (V); P_{in} is the incident light power (mW cm^{-2}); and J_{max} (mA cm^{-2}) and V_{max} (V) are the current density and voltage in the *I–V* curves, respectively, at the point of maximum power output.

RESULTS AND DISCUSSION

Morphology and Structural Characterization of PVdF–PAN-ESFM

Morphology. The FESEM image of the electrospun PVdF–PAN-ESFM is shown in Figure 2. For comparision, the FESEM images of PVdF and PAN are presented in Figure 2(a) and (b). The electrospun membranes have a three-dimensional fibrous interconnected network arrangement with high porosity. It consists of thin and smooth fibers with an average diameter of about 758 nm. The interconnected network structure of PVdF–PAN–ESFMs may be due to the presence of electrostatic force between electron withdrawing (C–F functional group of PVdF) and electron releasing (C–N functional group of PAN) groups.[16] There may be a possibility for the molecular interactions inducing the phase mixing between PVdF and PAN. Thus, the derived fiber was capable of uptaking adequate amount of electrolyte solution in its pores and has enough mechanical strength due to its three-dimensional network structure with numerous physical cross-linking points. The prepared electrospun composite fibers were smooth and free from bead-like structures. The reason may be due to the high polarity of DMF, low volatility of acetone, and polar nature of used polymer during polarization.[24]

X-Ray Diffraction (XRD) Pattern of PVdF–PAN-ESFM. To investigate the microscopic structure and the crystalline nature of electrospun PAN, PVdF, and PVdF–PAN-ESFM fibers, XRD measurements were performed. Figure 3 shows the XRD pattern of electrospun fiber. PVdF could crystallize in four polymorphs (α, β, γ, and δ) and each crystal structure had different polymorphs.[21] The crystallinity phases of the nanofiber membranes were investigated by means of X-ray diffraction [XRD; Figure 3(a)]. A strong diffraction peak for PVdF samples was observed at $2\theta = 20°$ which corresponds to the planer spacing "*d*" = 4.330 Å, which indicated the β phase of PVdF membrane.[25] The diffraction peak of the PAN fibers [Figure 3(b)] occurs at $2\theta = 18°$, which corresponds to the planar spacing

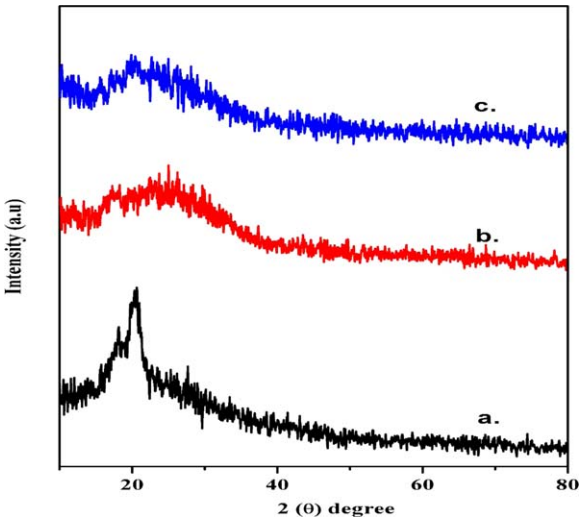

Figure 3. The XRD pattern of (a) PVdF, (b) PAN, and (c) PVdF–PAN. [Color figure can be viewed in the online issue, which is available at wileyonlinelibrary.com.]

$d = 5.03$ Å and can be indexed to the (100) plane of a hexagonal structure,[26] Figure 3(c) shows the amorphous nature of PVdF–PAN-ESFM peak intensity at $2\theta = 20.5°$ which corresponds to the planer spacing "d" = 4.3387 Å. The composite XRD pattern indicated that the PAN peaks totally shifted from hexagonal to crystal phase.

Most commonly, PAN crystals show two diffraction peaks around 17° and 29°. For dry PAN hexagonal lattice is a normal one.[27] Figure 3(C) shows only one broad peak in the region 20° and there is no peak observed around 29°. Hence it is concluded that the diffraction peak of PAN is hidden by PVdF because PAN is only 25 wt % in this composite.

Fourier Transform Infrared Spectroscopy (FTIR). The characteristic infrared spectral analysis was carried out for surface characterization of the nanofiber membranes in the range of 400–4000 cm^{-1} and is illustrated in Figure 4. For the electrospun PVdF fibers, Figure 4(a) shows the peak at about 1395.56, 1185.29, 867.74, and 485.26 cm^{-1}. The peaks at 1395.56, 867.74, and 485.26 cm^{-1} are due to the C–F_2 bending, wagging, and stretching vibration, and the peak at 1185.29 cm^{-1} is due to the C–C bond of PVdF.[1,28] Figure 4(b) shows the PAN-ESFM spectral peak at about 2934.32 which is assigned to the methylene (–CH_2) and –CH stretching vibration of the group. The peak at 2242.93 cm^{-1} frequency is due to nitrile (–CN) stretching mode. The peak at 1452.30 cm^{-1} is due to the bending vibration of methylene group.[1,26] One solvent peak at 1664.32 cm^{-1} of DMF appeared, which may be attributed to the vibration of the carbonyl (C=O) bond formed in the hydrolyzed PAN nanofibers and the stretching vibration of the carbonyl bonds in residual DMF solvent.[29] The composite nanofiber PVdF–PAN-ESFM membranes show bands corresponding to CF_2 vibrations [Figure 4(c)]. However, band subsequent to bending mode vibration shifted to 1398.30 cm^{-1} (1395.56 cm^{-1} in PVdF) in the spectrum of PVdF–PAN-ESFMs. Further, band positions of wagging mode of CF_2 are found to be shifted to higher frequency with a decrease in the intensity, as compared to the bands in PVdF. Typically, the band of C–F stretch at 1184.29 cm^{-1} is shifted to higher frequency. In addition, FTIR spectra of composites show bands around 3315.41, 3195.83, 2975.96, 2248, and 1670 cm^{-1} which correspond to the symmetrical –NH, –OH, –CH_2, –CN, and asymmetrical –CH stretching vibrations of PAN, respectively. Thus, these

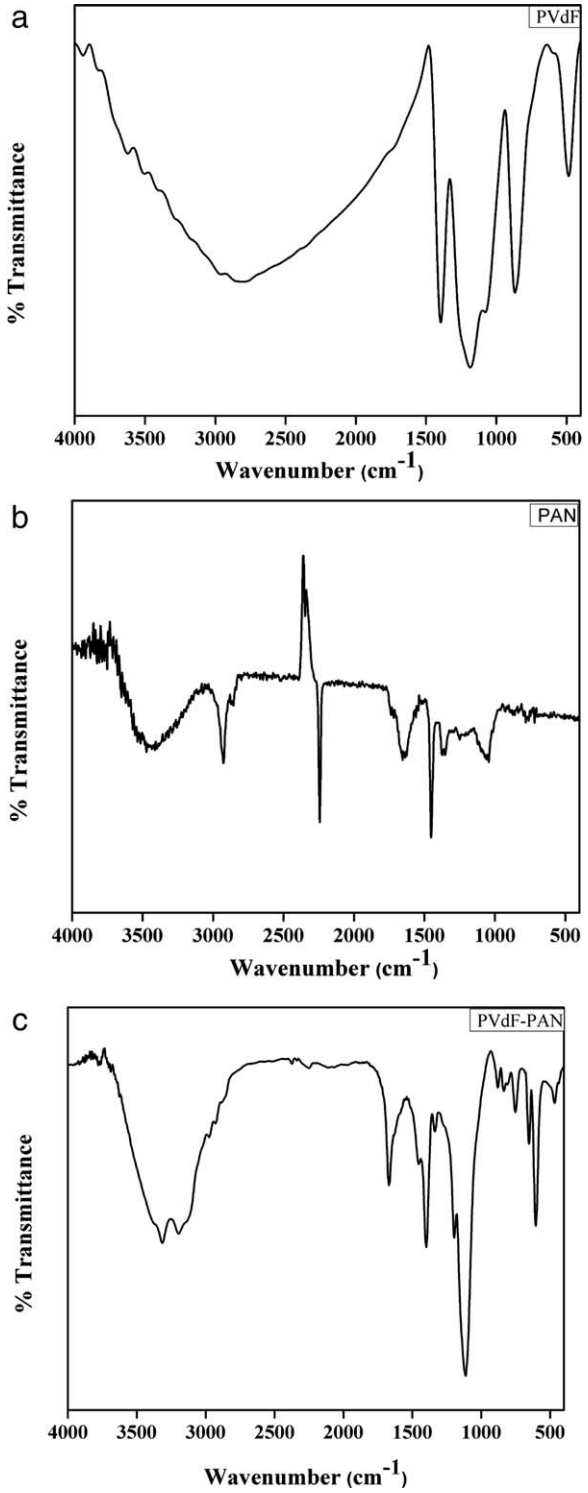

Figure 4. FT-IR spectra of (a) PVdF, (b) PAN, and (c) PVdF–PAN.

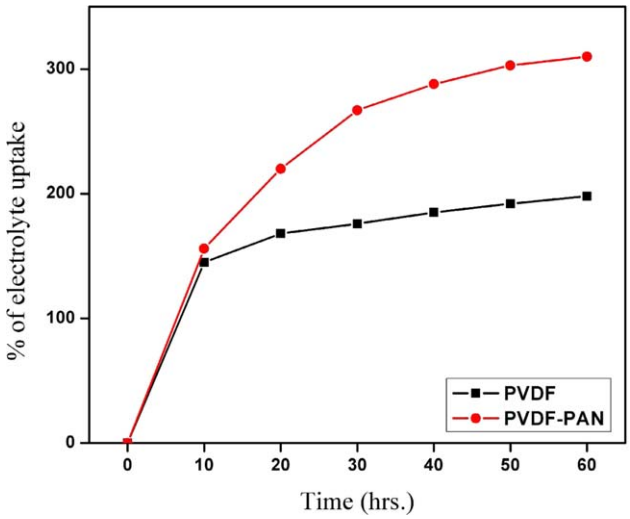

Figure 5. Electrolyte uptake characteristics of PVdF–PAN. [Color figure can be viewed in the online issue, which is available at wileyonlinelibrary.com.]

explanations clearly showed that there are molecular level interactions between the two polymers in the composite fibers.[1]

Electrolyte Solution and Uptake Performance. Figure 5 shows the electrolyte uptakes of the electrospun nanofiber membranes. The data was obtained by soaking the nanofiber membranes in the liquid electrolyte of 0.6*M* 1-hexyl-2,3-dimethylimidazolium iodide, 0.1*M* LiI, 0.05*M* I_2, and 0.5*M* 4-*tert*-butylpyridine in EC/PC (1 : 1 wt %) for a period of 1 h. The electrolyte uptake is observed to increase steadily with the PVdF–PAN-ESFMs fibers. The electrolyte uptake % of PVdF alone was 200%. When it is incorporated with PAN fiber, the PVdF–PAN-ESFMs fiber shows higher uptake of about 310.0%. Thus, the absorption of the huge amounts of liquid electrolyte by the electrospun-composite nanofiber membranes results from the high porosity of the membranes and the high amorphous content of the polymer. Furthermore, possibly, the completely 3D interconnected pore structure makes fast diffusion of the liquid into the membrane, and hence, the uptake process is alleviated within the initial 10–20 min.[20,21]

Porosity Measurements. Membranes with high porosity are suitable for incorporation of large amounts of liquid electrolyte and can attain high ionic conductivity at room temperature.[21]. The prepared electrospun composite membrane has 83.6% porosity which may be due to their well-developed interstices by the interconnected porous structure of nanofibers. The porosity of the nanofiber membranes influenced the relative polymer mass concentration.[20,30] As earlier electrolyte uptake result was about 310%, the reason behind this large increase in the uptake is, together with higher degree of porosity. Thus, the membranes with higher degree of porosity enhance the surface area of the pore that result in the higher uptake of the electrolyte solution. Therefore, the porosity plays an important role in the electrolyte uptake process. The composite was powdered and passed through a sieve with apertures equal to 1.0 mm. About 10 g of this material was introduced without compacting in to a measuring jar. The powder was carefully leveled and the volume was measured. The following formula was used to find the bulk density of polymer.[31]

$$M/V = D$$

where M is the mass of the polymer composite (g), V the volume of the polymer composite (mL), and D the density of the polymer composite.

Impedance Study for Ionic Conductivity of PVdF–PAN-ESFMs. The ionic conductivities of the electrospun-nanofiber membranes were measured at room temperature by the AC impedance method. Figure 6 shows the AC impedance data of PVdF,

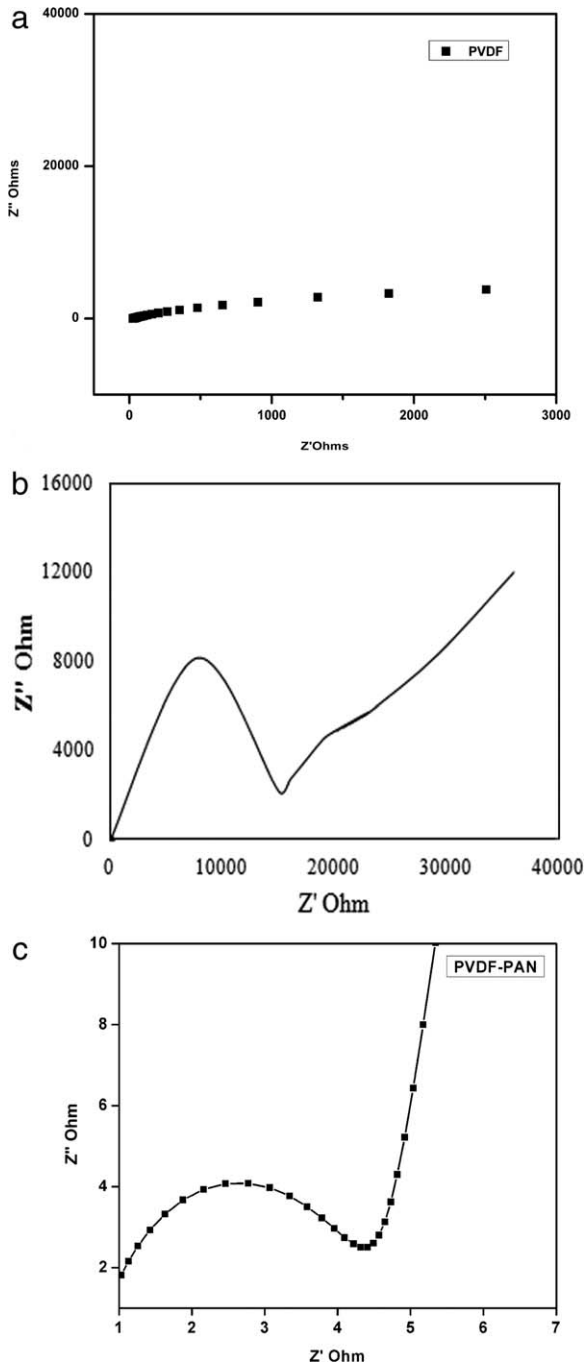

Figure 6. The ionic conductivity of (a) PVdF, (b) PAN, and (c) PVdF–PAN.

Table I. Comparison of Photovoltaic Performances of DSSCs Devices Using Electrospun PVdF–PAN Nanofiber Membrane

Electrolyte	Electrolyte J_{sc} (mA cm^{-2})	V_{oc} (V)	FF	η (%)	References
PEO electrolyte	1.88	0.63	50.7	0.60	30
PEO-KI-I_2	6.12	0.59	0.56	2.04	31
PBA/NaI/I_2	0.65	0.54	0.48	1.66	32
PVDF-HF (KI-EC-PC)	8.16	0.76	0.35	2.20	33
PEO/TiO_2	3.71	0.75	0.59	1.68	34
Liquid electrolyte	7.20	0.75	0.66	3.60	This study
PVDF-PAN	6.20	0.74	0.65	3.09	This study

PAN, and PVdF–PAN-ESFM polymer electrolytes respectively. The ionic conductivity mainly depends on the structure of pore size that absorbed liquid electrolytes and consequently the formation of pores in membranes is very essential for getting hold of proper channel of ionic conduction.[32] The ionic conductivities of PVdF [Figure 6(a)], PAN [Figure 6(b)], and PVdF–PAN-ESFM [Figure 6(c)] sample were observed 0.024 mS cm^{-1}, 2.27 mS cm^{-1} and 6.12 $\times$ 10^{-2} S cm^{-1}, respectively. The higher conductivity of PVdF–PAN-ESFM may be due to the interwoven structure introduced during electrospinning. The enhancement of ionic conductivity in composite polymer electrolytes has been attributed mainly to the decreased polymer crystallinity in the presence of interactions between the electrolyte polar groups of PVdF and PAN.[33,34] In addition, the interconnected 3D networks in the PVdF–PAN-ESFMs hindered the leakage of the liquid electrolyte.

DSSCs Photovoltaic Performances. The DSSCs device was equipped using the electrospun PVdF–PAN-ESFM nanofibers and their photovoltaic effects were investigated during the study. The PVdF–PAN composite fibers have good conductivity, porosity, and electrolyte uptake and hence they are considered to be good quasi-solid-state membrane for DSSCs. The diameter and morphology have not influenced the photovoltaic performances of DSSCs cells. The corresponding photovoltaic parameters like $J_{sc} = 6.20$ mA cm^{-2}, $V_{oc} = 0.74$ V, FF = 0.65, and efficiency ($\eta = 3.09\%$) of the DSSC devices using electrospun PVdF–PAN-ESFM were determined and summarized in Table I and the *I–V* graph is shown in Figure 7. This photovoltaic efficiency is comparable with that observed for liquid electrolytes (3.60%) and is higher than that reported recently for similar systems, 0.60, 2.04, 1.66, and 2.20 (1.68%).[35–39]

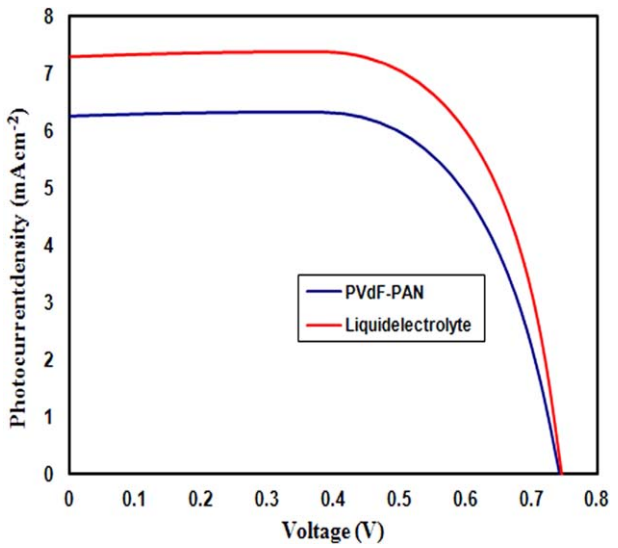

Figure 7. *I–V* curves of DSSCs device using electrospun PVdF–PAN nanofiber membrane. [Color figure can be viewed in the online issue, which is available at wileyonlinelibrary.com.]

CONCLUSIONS

The PVdF–PAN nanofibrous membrane was prepared from a solution of PVdF and PAN by electrospinning method. The polymer electrolyte was prepared by soaking the membrane in the electrolyte solution. Three-dimensional interconnected network regular morphology with large number of voids and cavities of different diameters observed from FESEM images resulted in 83.6% porosity and this helps higher uptake of the electrolyte (310%). The ionic conductivity determined is 6.12 $\times$ 10^{-2} S cm^{-1}. Employing the polymer electrolyte, DSSCs were fabricated successfully and their photovoltaic performances were evaluated. The solar-to-light electricity conversion efficiency of the quasi-solid-state solar cells with the electrospun PVdF–PAN-ESFM membrane electrolyte was 3.09%, which was comparable to that of 3.60% observed for the liquid electrolyte and higher than the observed values from reports.

ACKNOWLEDGMENTS

This work was supported by the funding agency of AURF, UGC-BSR and DST-PURSE. The authors acknowledge the School of Physics, Alagappa University, Karaikudi, for XRD and the Central Electro Chemical Research Institute (CECRI), Karaikudi, for *I–V* measurements.

REFERENCES

1. Ahn, S. K.; Ban, T.; Sakthivel, P.; Lee, J. W.; Gal, Y. S.; Lee, J. K.; Kim, M. R.; Jin, S. H. *ACS Appl. Mater. Interfaces* **2012**, *4*, 2096.
2. Gratzel, M. *Acc Chem. Res.* **2009**, *42*, 1788.
3. Gratzel, M. *J. Photoch. Photobiol. A* **2004**, *164*, 3.
4. Paruthimal Kalaignan, G.; Moon-Sung, K.; Young Soo, K. *J. Solid State Ionics* **2006**, *177*, 1091.

5. Hongxun, Y.; Miaoliang, H.; Jihuai, W.; Zhang, L.; Sancun, H.; Jianming, L. *J. Mater. Chem. Phys.* **2008**, *110*, 38.
6. Ying, Y.; Cong-hua, Z.; Sheng, X.; Hau, H.; Bo-lei, C.; Jing, Z.; Su-Juan, W.; Wei, L.; Xing-zhong, Z. *J. Power Sources* **2008**, *185*, 1492.
7. Yella, A.; Lee, H. W.; Tsao, H. N.; Yi, C. Y.; Chandiran, A. K.; Nazeeruddin, M. K.; Diau, E. W. G.; Yeh, C. Y.; Zakeeruddin, S. M.; Gratzel, M. *Science* **2011**, *334*, 629.
8. Mohmeyer, N.; Wang, P.; Schmidt, H. W.; Zakeeruddin, S. M.; Gratzel, M. *J. Mater. Chem.* **2004**, *14*, 1905.
9. Wang, P.; Zakeeruddin, S. M.; Humphry-Baker, R.; Gratzel, M. *Chem. Mater.* **2004**, *16*, 2694.
10. Nageswaran, S.; Raghavan, P.; Hng, H. H.; Srinivasan, M. *Mater. Res. Bull.* **2013**, *48*, 526.
11. Kim, J. Y.; Kim, T. H.; Kim, D. Y.; Park, N. G.; Ahn, K. D. *J. Power Sources* **2008**, *175*, 692.
12. Subramania, A.; Sundaram, N. T. K.; Kumar, G. V. *J. Power Sources* **2006**, *153*, 177.
13. Chen, C.; Wang, L.; Huang, Y. *Appl. Energy* **2011**, *88*, 3133.
14. Mthethwa, T. P.; Moloto, M. J.; De Vries, A.; Matabola, K. P. *Mater. Res. Bull.* **2011**, *46*, 569.
15. SathiyaPriya, A. R.; Subramania, A.; Jung, Y. S.; Kim, K. *J. Langmuir* **2008**, *24*, 9816.
16. Gopalan, A. I.; Padmanabhan, S.; Manesh, K. M.; Nho, J. H.; Kim, S. H.; Hwang, C. G.; Lee, K. P. *J. Membr. Sci.* **2008**, *325*, 683.
17. Raghavan, P.; Vanchiappan, A.; Srinivasan, M. *J. Power Sources* **2012**, *202*, 299.
18. Wang, L.; He, X.; Li, J.; Chen, M.; Gao, J.; Jiang, C. *Electrochim. Acta.* **2012**, *72*, 114.
19. Park, S. H.; Wona, D. H.; Choi, H. J.; Hwang, W. P.; Jang, S.; Kim, J. H.; Jeong, S. H.; Kim, J. U.; Lee, J. K.; Kim, M. R. *Sol. Energ. Mat. Sol. C.* **2011**, *95*, 296.
20. Raghavan, P.; Zhao, X.; Shin, C.; Baek, D. H.; Choi, J. W.; Manuel, J.; Heo, M. Y.; Ahn, J. H.; Nah, C. *J. Power Sources* **2010**, *195*, 6088.
21. Kose, R.; Mitani, I.; Kasai, W.; Kondo, T. *Biomacromolecules* **2011**, *12*, 716.
22. Chen, C. L.; Teng, H.; Lee, Y. L. *J. Mater. Chem.* **2010**, *21*, 628.
23. Ding, Y.; Zhang, P.; Long, Z.; Jiang, Y.; Xu, F.; Wei, D. *Sci. Technol. Adv. Mater.* **2008**, *9*, 015005.
24. Dong, H.; Nyame, V.; MacDiarmid, A. G.; Jones, W. E. J. *J. Polym. Sci. Part B: Polym. Phys.* **2004**, *42*, 3934.
25. Chung, M. Y.; Lee, D. C. *J. Korean Phys. Soc.* **2001**, *38*, 117.
26. Panapoy, M.; Dankeaw, A.; Ksapahutr, B. *Thammasat. Int. J. Sci. Tech.* **2008**, *13*, 11.
27. Lianjiang, T.; Huifang, C.; Ding, P.; Ning, P. *Eur. Polym. J.* **2009**, *45*, 1617.
28. Jin, K. Y.; Ahn, C. H.; Lee, M. B.; Choi, M. S. *Mater. Chem. Phys.* **2011**, *127*, 137.
29. Choi, S. W.; Kim, J. R.; Jo, S. M.; Lee, W. S.; Kim, Y. R. *J. Electrochem. Soc.* **2005**, *152*, A989.
30. Costa, C. M.; Rodrigues, L. C.; Sencadas, V.; Silva, M. M.; Rocha, J. G.; Lanceros-Méndez, S. *J. Membr. Sci.* **2012**, 193–201, *407*.
31. USP35. http://www.usp.org/sites/default/files/usp_pdf/EN/USPNF/revisions/m99375 (accessed August 31, **2013**).
32. Lee, J. K.; Choi, H. J.; Park, S. H.; Won, D. H.; Park, H. W.; Kim, J. H.; Lee, C. J.; Jeong, S. H.; Kim, M. R. *Mol. Cryst. Liq. Cryst.* **2010**, *519*, 234.
33. Chung, S. H.; Wang, Y.; Persi, L.; Croce, F.; Greenbaum, S. G.; Scrosati, B.; Plichta, E. *J. Power Sources* **2001**, *97/98*, 644.
34. Santhosh, P.; Vasudevan, T.; Gopalan, A.; Lee, K. P. *Mater. Sci. Eng. B.* **2006**, *135*, 65.
35. Singh, P. K.; Kim, K. I.; Park, N. G.; Rhee, H. W. *Macromol. Symp.* **2007**, 249–250, *162*.
36. Kalaignan, G. P.; Kang, M. S.; Kang Y. S. *J. Solid State Ionics* **2006**, *177*, 1091.
37. Kim, J. H.; Kang, M. S.; Kim, Y. J.; Won, J.; Kang, Y. S. *J. Solid State Ionics* **2005**, *176*, 579–584.
38. Noor, M. M.; Buraldah, M. H.; Yusuf, S. N. F.; Careem, M. A.; Majid, S. R.; Arof, A. K. *Int. J. Photoenergy* **2011**, 2011, 1.
39. Singh, P. K.; Bhattacharya, B.; Nagarale, R. K. *J. Appl. Polym. Sci.* **2010**, *118*, 2976.